IOSR Journal of VLSI and Signal Processing (IOSR-JVSP)
Volume 5, Issue 6, Ver. II (Nov -Dec. 2015), PP 16-24
e-ISSN: 2319 – 4200, p-ISSN No. : 2319 – 4197
www.iosrjournals.org

Single image super resolution with improved wavelet interpolation and iterative back-projection

Boniface M. Ngocho, Elijah Mwangi
School of Engineering, University of Nairobi. PO BOX 30197 Nairobi 00100, Kenya

Abstract : *Spatial resolution of digital images is limited by practical considerations of digital imaging systems. Single image super resolution is therefore required to create images that allow better identification and interpretation of details. A number of investigations have been carried out on image super resolution using the discrete wavelet transform. In this paper, a comparative study is made of different interpolation based methods for the estimation of high frequency sub-bands for the super resolution image. An investigation of the effect of different parameters in bicubic interpolation kernel is also carried out. Based on the result, a new algorithm is proposed for single image super resolution using the discrete wavelet transform and incorporating iterative back-projection. The proposed method is tested against other approaches and found to give superior results in terms of peak signal to noise ratio and structural similarity index measure.*

Keywords: *Super resolution, wavelets, bicubic interpolation, iterative back-projection*

I. INTRODUCTION

Digital imaging systems have a wide variety of applications for commercial, medical and recreational purposes. In many of these applications, a high quality image is required to allow human interpretation or machine perception. However, the spatial resolution of digital images is sometimes limited by technical considerations of the imaging system or the environmental conditions in which the image is captured. This has led to the need for signal processing techniques to create a higher resolution image that will allow better identification and interpretation of details.

The aim of single image super resolution is to create a high resolution image from a single instance of a low resolution image of the original scene. Among the popular methods are direct interpolation, estimation of the missing data using statistical methods, use of wavelets and example based procedures.

In spatial domain interpolation, the pixel values of a low resolution image are extrapolated to fit a high resolution grid using an interpolation kernel. Commonly used interpolation kernels are nearest neighbour, bilinear interpolation, bicubic interpolation and windowed sinc functions [1], [2], [3], [4]. The cubic B-spline is another interpolation method that has been found to produce better results than most other interpolation kernels. The kernel however does not directly interpolate the pixels of the low resolution image. The implementation of B-spline interpolation therefore requires a two-step process which leads to an increase in computation time. This has resulted in bicubic interpolation getting more widespread application than cubic B-spline interpolation [1].

In wavelet based super resolution, the available LR image is assumed to be the low frequency sub-band, *LL*, of a high resolution image. The resolution task is to estimate the high resolution sub-bands in order to complete the image. Tsai and Acharya proposed to use the Stationary Wavelet Transform (SWT) of the LR image to provide the high resolution sub-bands [5]. Since the SWT is not decimated, the *LH*, *HL* and *HH* sub-bands will have the same size as the LR image. Implementing Inverse Discrete Wavelet Transform (IDWT) will therefore result in image with twice the number of rows and columns. Temizel and Vlachos used a similar approach in which high resolution sub-bands are derived from un-decimated SWT coefficients [6]. Other approaches combined SWT and Discrete Wavelet Transform (DWT) to achieve higher Peak Signal to Noise Ratio (PSNR) than SWT alone [7], [8], [9], [10]. In [8], DWT decomposition is carried out on bicubic interpolated LR image. In [7] and [9], high frequency sub-bands are obtained through bicubic interpolation of DWT sub-bands of the LR image. Bicubic interpolation followed by DWT without combination with SWT is applied in [11] and [12]. A number of investigations have proposed the incorporation of edge enhancement in the reconstruction of high frequency sub-bands [13], [14], [15]. Carey et al [13] used multiple levels of DWT decomposition to identify strong edges. The rate of decay of the edges was then used to estimate the unknown high frequency sub-bands. Kwon and Park [16] propose a support vector machine to synthesize the high frequency sub-bands from the DWT decomposed low resolution image without use of interpolation.

Single image super resolution is an ill-defined inverse problem without a unique solution. Application of additional constraints in the process can limit the number of possible outcomes and achieve results that are closer to the ground truth. One such process is Iterative Back-Projection (IBP), first proposed for application in image super resolution by Irani and Peleg [17]. This has been subsequently applied in other investigations. Dai

et al applied back-projection together with bilateral filtering to achieve enhanced edges [18]. Filter based edge enhancement methods are also applied in [19] and [20].

This investigation compares the different methods of estimating the high frequency sub-band to identify the one that gives the best results in terms of both PSNR and Structural Similarity Index Measure (SSIM). The investigation is limited to approaches that require only one level of DWT decomposition.

The rest of this paper is arranged as follows. Section II contains the background on related work and contribution made in this investigation. Section III presents the proposed super resolution method. Section IV presents results of simulations carried out in the process of developing the resolution algorithm. This includes results for parts of the algorithm as well as results for the complete process. Section V presents conclusions of the investigation and suggested future work.

II. RELATED WORK & CONTRIBUTION

2.1. Bicubic Interpolation

The bicubic interpolation is based on an interpolation kernel proposed by Keys [4] and is given in (1):

$$u(s) = \begin{cases} (a+2)|s|^3 - (a+3)|s|^2 + 1 & 0 \le |s| < 1 \\ a|s|^3 - 5a|s|^2 + 8a|s| - 4a & 1 \le |s| < 2 \\ 0 & 2 \le |s| \end{cases} \tag{1}$$

$$g(x) = \sum_k f(k)u(x-k) \tag{2}$$

This kernel is applied in (2) in order to interpolate new values of a super resolution image, *g(x)* from existing values of a low resolution image, *f(k)*. The constant, *a*, is a variable of unknown value. In order for the kernel to achieve the general shape of the sinc function, *a* must lie between -3 and 0. Keys [4] defined *a* as -0.5 in order to achieve third order convergence of Taylor's series for the interpolation kernel. However, Taylor's series assumes a smooth function that is continuously differentiable, which may not be true for images. In later reviews of interpolation methods [2], [3], it has been noted that a value of -1 for *a* achieves continuity in the first derivative of *u(s)* at *s*=1. A value of -0.75 achieves continuity of the second derivative.

In this investigation, the value of *a* that will result in the best interpolation performance is determined experimentally. The performance is measured in terms of PSNR and SSIM.

2.2. Wavelet Based Super Resolution

In wavelet multiresolution using the Discrete Wavelet Transform (DWT) a signal is divided into two components, *L* and *H*, each containing half of the frequencies in the original signal. *L* contains the low frequencies while *H* contains the high frequencies. This is represented in (3) and (4) where x[n] is the input signal, φ is the scaling function, ψ is the wavelet function and the operation < > represents vector (inner) product:

$$L = \langle \varphi_{1,k}, x[n] \rangle = \sum_{k=-\infty}^{\infty} \varphi_{1,k}^{*}\, x[n] \tag{3}$$

$$H = \langle \psi_{1,k}, x[n] \rangle = \sum_{k=-\infty}^{\infty} \psi_{1,k}^{*}\, x[n] \tag{4}$$

For a two dimensional image, the decomposition is done in two steps, along rows followed by along columns. The first steps yields *L* and *H* while the second step will decompose *L* into *LL* and *LH* and *H* into *HL* and *HH*. This results in the decomposition of the image into 4 sub-bands based on frequency content, as shown in Fig. 1.

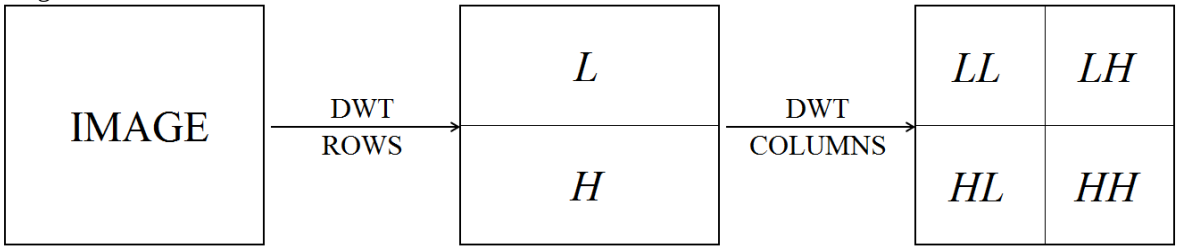

Figure 1. DWT Multi-resolution decomposition

In wavelet based super resolution, the available LR image is assumed to be the low frequency sub-band, *LL*, of a high resolution image. The problem, as in Fig. 2, is to estimate the high resolution sub-bands in order to construct the image.

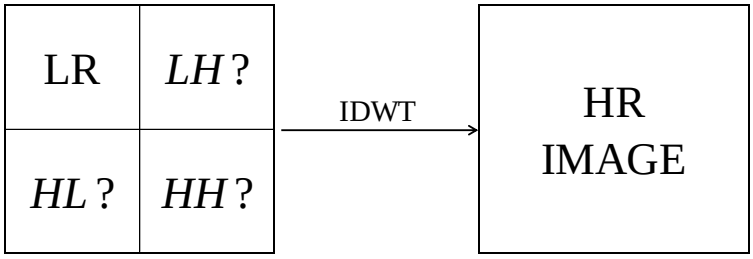

Figure 2. Wavelet Super Resolution Concept

It is noted in the introduction that a number of approaches have been made for the estimation of the high frequency sub-bands. This study will evaluate the performance of different interpolation based approaches and select the estimation method that results in best performance in super resolution.

2.3. Iterative Back-projection

Single image super resolution is an ill posed inverse problem. Application of additional constraints in the process can limit the number of possible outcomes and achieve results that are closer to the ground truth. One such process is iterative back-projection. This is a process applied in computed tomography (CT) to reconstruct 3D images from multiple 2D images. The process has been adapted for application in image super resolution [17], [18]. Iterative back-projection starts with an initial super resolution image, SR_n. This is down-sampled to produce a low resolution image, $SR_n\downarrow$ which is subtracted from the original low resolution image, LR, to obtain reconstruction error, *e*. This error is up-sampled and added to SR_n to obtain a new high resolution image, SR_{n+1}. This process is repeated until the iteration converges. The process is summarised in (5):

$$e_n = LR - SR_n\downarrow$$
$$SR_{n+1} = SR_n + e_n\uparrow \quad (5)$$

Where a down arrow represents down-sampling by a factor of 2 while an up arrow represents up-sampling by a factor of 2.In this investigation, IBP has been applied to the results of the wavelet based super resolution process. Measurement of PSNR and SSIM on each new super resolution image is used to determine the number of steps required before the iteration converges.

III. PROPOSED METHOD

The proposed method combines wavelet based super resolution and iterative back-projection to achieve single image super resolution. A spatial domain interpolation technique is used to estimate the missing high frequency sub-bands of the SR image. The resulting image is then subjected to iterative back-projection to minimize reconstruction error. Wavelet decomposition and reconstruction is carried out using Haar wavelet.

A flow chart of the proposed algorithm is given in Fig. 3. The input is a low resolution image, which is subjected to two parallel operations.

In the first operation, the image is subjected to a mathematical operation whereby each pixel value is multiplied by a factor λ in order to match the wavelet transform normalisation factor. This results in a new image *LR*'.

In the second operation, the LR image is interpolated by a factor of 2 using bicubic interpolation. The interpolated image is then decomposed into four quadrants using discrete wavelet transform.

The results of the two operations are used as inputs in the next stage of the process. The *LL* quadrant is discarded and replaced with the modified input image, *LR*'. This, together with the *LH*, *HL* and *HH* quadrants are used as inputs for the reconstruction of the first level super resolution image, SR_0 image using the Inverse Discrete Wavelet Transform (IDWT).

The resultant super resolution image is taken to the last stage, which is application of the iterative back-projection technique. This involves:

1. Down-sampling the latest SR_n image using decimation of rows and columns to create a new low resolution image, LR_n image.
2. Subtracting the latest LR_n image from the original input image, *LR* to create an error image, e_n.
3. Up-sampling the error image using wavelet zero padding.
4. Adding the up-sampled error image to the last SR image, SR_n to create a new SR image, SR_{n+1}.

5. Repeating process until iteration converges.

The output after convergence of back-projection is the final super resolution image.

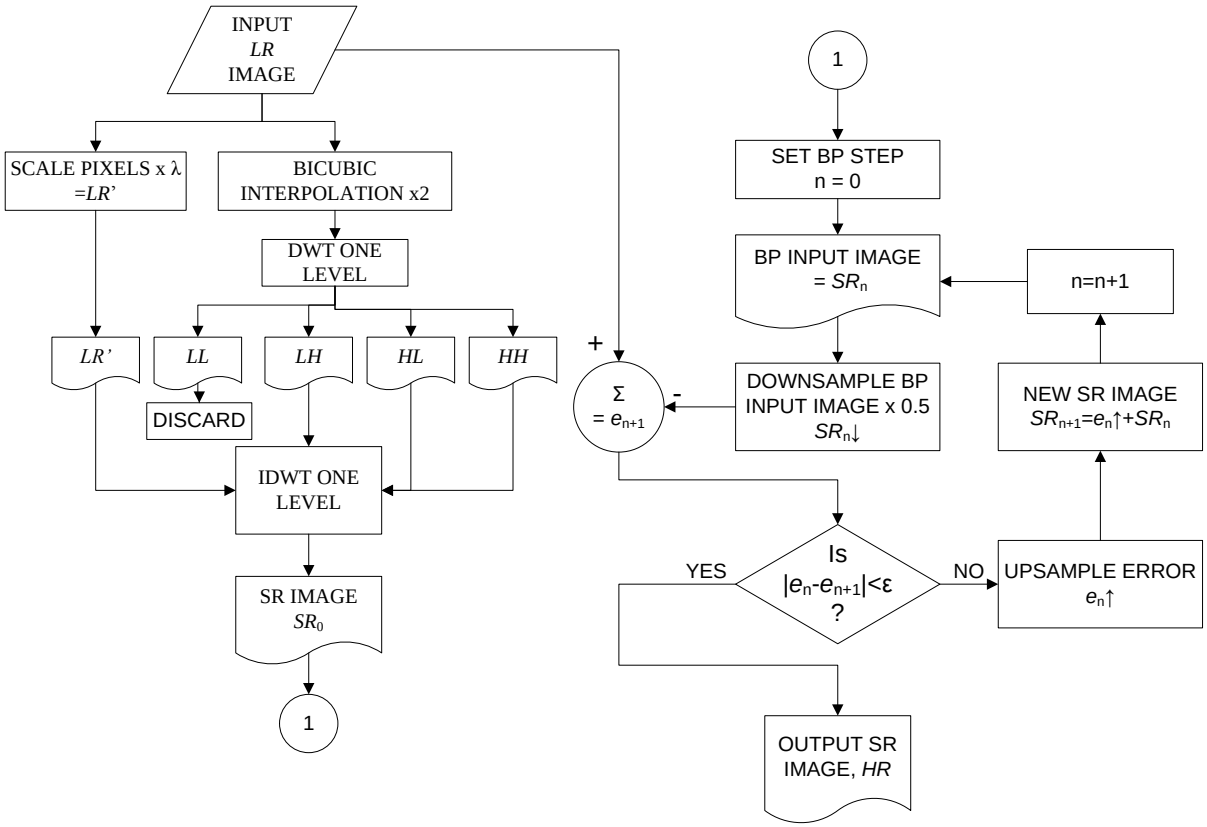

Figure 3. Flow chart for proposed algorithm

IV. RESULTS & DISCUSSIONS

In formulating the algorithm, each stage is developed and tested separately before the final algorithm is implemented and tested. Testing is carried out in Matlab. Images used are from the Kodak True Colour Lossless Images collection. The images used in development are *Kodim07 (Window); Kodim13 (Stream); Kodim15 (Girl); Kodim19 (Lighthouse) and Kodim23 (Parrots).* For the purposes of this study, the level of super resolution is limited to a factor of 2 on rows and columns. Testing of parts of the algorithm is carried out on greyscale images. The proposed algorithm is tested on RGB colour images.

4.1. Performance Measures

Performance measures for image super resolution require comparison of SR image and the actual scene. In order to implement such an approach, the starting point is a high resolution image which will be considered to be the ground truth image. The ground truth image is down-sampled to produce a Low Resolution (LR) image which is the input to the super resolution process. The output of the super resolution process is the SR image, which is compared with the ground truth image in order to measure performance of the process.

The most common performance measure is Peak Signal to Noise Ratio (PSNR), which compares the errors in pixel values between the ground truth image and super resolution image as summarised in (6) and (7):

$$MSE = \frac{\sum_i \sum_j \left(\left(GT(i,j) - SR(i,j) \right) \right)^2}{I * J} \tag{6}$$

$$PSNR = 10 * log_{10} \left(\frac{L^2}{MSE} \right) \tag{7}$$

In (6), the computation of the mean square error, *MSE* is presented. *GT(i,j)* is the value of the pixel at location *(i,j)* in the ground truth image while *SR(i,j)* is the value of the pixel at location *(i,j)* in the super resolution image. *I* and *J* are the total number of rows and columns respectively in each image. In (7), the *PSNR* is computed by dividing L^2 by the mean square error (*MSE*). *L* is the dynamic range of pixel value, which is 255

for 8-bit encoded images.

The main shortcoming of PSNR as a measure of image quality is lack of any correlation between the measure and human perception of an image. An image quality measure that attempts to correct this shortcoming is the Structural Similarity Index Measure (SSIM) [21]. The computation of SSIM is as given in (8):

$$SSIM(x,y) = \frac{(2\mu_x\mu_y + C_1)(2\sigma_{xy} + C_2)}{(\mu_x^2 + \mu_y^2 + C_1)(\sigma_x^2 + \sigma_y^2 + C_2)} \tag{8}$$

Where, x and y are the images whose structural similarity is to be evaluated. μ_x is the mean luminance of image x while μ_y is the mean luminance of image y. σ_x and σ_y are the signal contrasts of images x and y respectively. σ_{xy} is the contrast between images x and y. C_1 and C_2 are constants chosen to avoid instability when one of the factors in the denominator is close to zero.

Both PSNR and SSIM are used as quality measures in this investigation.

4.2. Reviewing Bicubic Interpolation

A plot of the bicubic interpolation kernel for different values of the constant a is shown in Fig. 4 and Fig 5. The plot in the spatial domain is in Fig. 4, while Fig. 5 presents the plot in the frequency domain.

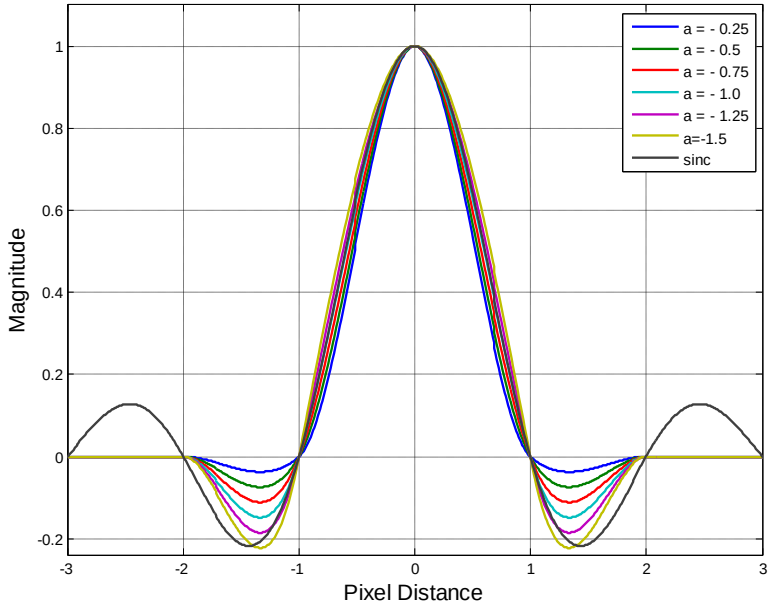

Figure 4. Cubic Interpolation Kernel – Spatial Domain

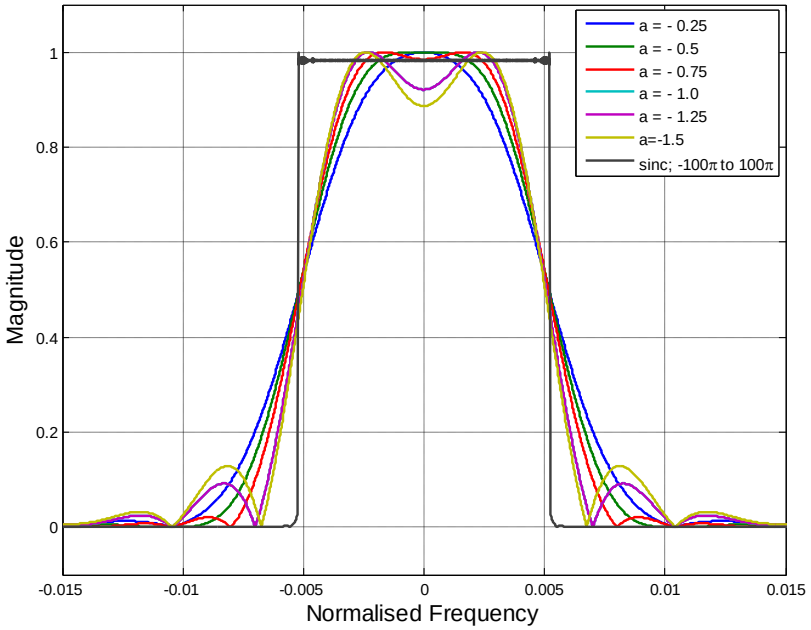

Figure 5. Frequency Response of Cubic Kernel

It is observed from Fig. 4 that in the spatial domain, the cubic kernel matches the sinc function more closely as the value of *a* becomes more negative. From Fig.5, the following observation can be made on the frequency response of the kernel:

1. In the pass band, the frequency response becomes wider at the top as the value of *a* becomes more negative. This will have the effect of increasing the gain in the pass band, hence improving the image quality.
2. In the stop band, the drop-off in gain is sharper as the value of *a* becomes more negative. This should help to reduce aliasing.
3. Also in the stop band, there are some additional lobes, which increase in magnitude as *a* becomes more negative. The extra gain will have the positive effect of sharpening edges of extrapolated image. It will also have the negative effect of increasing aliasing.

These observations suggest that there is a certain value of *a* where the effects will balance out and the best possible output is obtained from the kernel. Table 1 shows the value of *a* which results in the maximum value of PSNR and SSIM when used in bicubic interpolation of the selected test images. Discarding the extreme values obtained for the image *Stream*, the mean of the remaining values of *a* is -1.33. This was adopted as the working value for bicubic interpolation in the proposed algorithm.

Table 1: Values of a for maximum PSNR / SSIM in bicubic interpolation

IMAGE		Window	Stream	Parrots	Lighthouse	Girl
MAXIMUM PSNR	***a***	-1.40	-1.10	-1.35	-1.25	-1.20
	PSNR, dB	32.27	23.13	33.7	27.29	30.59
MAXIMUM SSIM	***a***	-1.35	-1.8	-1.25	-1.45	-1.35
	SSIM	0.943	0.709	0.948	0.839	0.892

4.3. Wavelet super resolution

It is noted from the introduction that there have been different interpolation based approaches to estimating the high frequency wavelet sub-bands for the super resolution image. In order to identify the best method, four methods and their combined use were applied in super resolution and the resultant images were compared in terms of PSNR and SSIM. In all cases, the input low resolution image is used as the *LL* sub-band of the super resolution image. The PSNR results are in Table 2 and the SSIM results in Table 3. The wavelet sub-band estimation methods tested are:

1. Wavelet Zero padding, where all the sub-bands are set to zero.
2. Use of high frequency sub-bands obtained from the Stationary Wavelet Transform (SWT).
3. The input low resolution image is interpolated by a factor of 2 using bicubic interpolation and the resultant image is subjected to DWT. The resultant high frequency sub-bands are used as the high frequency sub-bands of the super resolution image.
4. The input low resolution image is subjected to DWT. The resultant high frequency sub-bands are interpolated by a factor of two using bicubic interpolation and used as the high frequency sub-bands of the super resolution image.
5. A combination of methods 2 and 3 is applied.
6. A combination of methods 2 and 4 is applied.
7. A combination of methods 3 and 4 is applied.

Table 2. PSNR (dB) Results for alternative Wavelet super resolution methods

METHOD	IMAGE				
	Girl	Lighthouse	Parrots	Stream	Window
1	29.76	26.65	31.50	22.38	29.72
2	26.78	24.63	29.30	20.92	27.68
3	**30.91**	**27.83**	**33.97**	**23.19**	**32.67**
4	28.70	24.47	30.88	20.97	29.30
5	29.14	26.86	31.98	22.56	30.53
6	28.77	25.87	31.32	22.00	29.76
7	30.46	26.73	33.09	22.58	31.63

Table 3: SSIM Results for alternative Wavelet super resolution methods

METHOD	IMAGE				
	Girl	Lighthouse	Parrots	Stream	Window
1	0.8835	0.8316	0.9318	0.6995	0.9144
2	0.8512	0.7980	0.9140	0.6606	0.8875
3	**0.9016**	**0.8567**	**0.9510**	**0.7416**	**0.9498**
4	0.8444	0.7761	0.9062	0.6306	0.8863
5	0.8884	0.8433	0.9416	0.7239	0.9318
6	0.8703	0.8194	0.9265	0.6921	0.9096
7	0.8865	0.8342	0.9391	0.7109	0.9319

It is observed from the results in Table 2 and Table 3 that for all the images, method number 3 produced the best performance of the super resolution, both in terms of PSNR and SSIM. This method involves bicubic interpolation of the input low resolution image followed by DWT multiresolution of the interpolated image. The resulting high frequency sub-bands, together with the input low resolution image, are used as the input in the IDWT to create the super resolution image.

4.4. Back-projection

Iterative back-projection was applied after the super resolution process selected in the previous section. It was observed that the error image after two steps of iterative back-projection contained no identifiable information. The number of steps required for convergence of IBP process is therefore two.

4.5. Proposed Algorithm

The proposed algorithm based on the selected wavelet super resolution approach and two steps of iterative back-projection is presented in Fig. 3. This method is applied to the 5 selected images. The algorithm is applied independently on each colour channel of the RGB colour images. The results are compared with the following methods:

1. Bicubic interpolation.
2. Wavelet zero padding.
3. Implementation of method proposed by Naik and Patel [8]. This method is based on wavelet super resolution but combines two methods for deriving the high frequency sub-bands. It also includes a smoothing filter after back-projection.
4. New Edge Directed Interpolation (NEDI). This is an edge directed algorithm proposed by Li and Orchard [22].

The results in terms of PSNR are in Table 4 while SSIM results are in Table 5. The highest value for PSNR and SSIM for each image are indicated in bold.

Table 4: PSNR Results for proposed algorithm

IMAGE / METHOD		PROPOSED			BICUBIC			NAIK &PATEL			NEDI		
		R	G	B	R	G	B	R	G	B	R	G	B
PSNR (dB)	**Girl**	**30.81**	**31.11**	**30.90**	30.62	30.75	30.71	29.69	29.90	29.74	25.25	25.34	25.65
	L.House	**27.96**	**27.81**	**27.98**	27.54	27.50	27.75	27.28	27.22	27.39	25.25	25.34	25.65
	Parrots	**33.91**	**33.82**	**34.58**	33.21	33.11	33.85	32.74	32.75	33.54	31.26	31.21	31.65
	Stream	**23.33**	**23.27**	**23.17**	23.23	23.15	23.11	22.78	22.73	22.59	22.00	21.89	21.89
	Window	**32.78**	**32.76**	**32.60**	32.10	32.08	32.00	31.54	31.54	31.45	29.35	29.24	29.29

Table 5: SSIM Results for proposed algorithm

IMAGE / METHOD		PROPOSED			BICUBIC			NAIK &PATEL			NEDI		
		R	G	B	R	G	B	R	G	B	R	G	B
PSNR (dB)	**Girl**	**0.898**	**0.906**	**0.890**	0.892	0.899	0.884	0.891	0.896	0.880	0.862	0.869	0.851
	L.House	**0.864**	**0.855**	**0.841**	0.851	0.842	0.828	0.855	0.847	0.833	0.804	0.798	0.784
	Parrots	**0.950**	**0.950**	**0.951**	0.948	0.947	0.948	0.944	0.944	0.945	0.933	0.932	0.931
	Stream	**0.737**	**0.751**	**0.709**	0.706	0.721	0.679	0.726	0.741	0.694	0.623	0.639	0.589
	Window	**0.949**	**0.950**	**0.947**	0.944	0.945	0.942	0.941	0.942	0.938	0.909	0.910	0.907

It is observed that in all cases, the proposed algorithm performs better than the comparative methods both in terms of PSNR and SSIM.

Selections of extracts from the images used are presented in Fig 6 to Fig 8. The extracts are from the ground truth image, the simulated low resolution image and the super resolution result by the proposed method. In Fig. 6, extracts from the *Lighthouse* image are presented. The louvres and picket fence show sharp edges in the ground truth image, which are very blurred in the low resolution image. The sharpness of the edges is partly recovered in the super resolution image.

In Fig. 7, extracts from the *Parrots* image are displayed. The details around the eye and features on the beak which are blurred and unclear in the low resolution image are recovered in the super resolution image.

Extracts from the image *Stream* are shown in Fig. 8. The key features here are the snow in the mountain valleys, which demonstrated the chequered board effect in the low resolution image. Also, the grey level of the mountain in the low resolution image does not appear to the same as in the high resolution image. These details undergo some correction in the high resolution image.

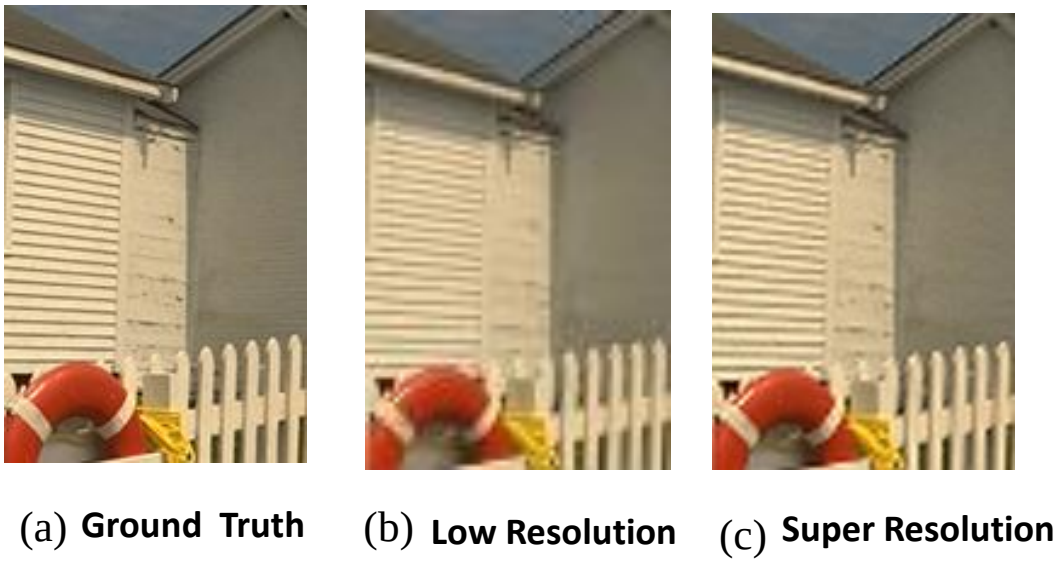

Figure 6: Zoomed in extracts from the image *Lighthouse*

Figure 7: Zoomed in extracts from the image *Parrots*

Figure 8: Zoomed in extracts from the image *Stream*

V. CONCLUSION

In this paper, the bicubic interpolation kernel as well as wavelet super resolution have been reviewed.

It has been demonstrated that it is possible to improve the performance of bicubic interpolation through the correct selection of the independent constant, *a*, in the interpolation kernel.

Different interpolation based methods of estimation of high frequency sub-bands in wavelet super resolution have also been investigated. It has been established that the method of first interpolating the low resolution image and then carrying out DWT of the interpolated image results in a better performance than all other interpolation based methods, used either alone or as a combination of two methods.

Finally, an algorithm that incorporates the findings as well as iterative back-projection has been formulated and tested. The algorithm has been tested on RGB colour images and has been demonstrated to produce better results than bicubic interpolation and the comparative methods tested.

It has been noted from the literature that cubic B-splines give better performance than cubic interpolation. It would therefore be useful to test whether a combination of cubic B-splines and wavelets can achieve better results than cubic B-splines alone. Wavelet analysis in this investigation was carried out using the Haar wavelet. Further investigation may establish whether performance improvements can be achieved by using other wavelets.

REFERENCES

[1] P. Thevenaz, T. Blu and M. Unser, "Image interpolation and resampling," in *Handbook of Medical Imaging*, 2 ed., I. Bankman, Ed., San Diego, California, Elsevier/Academic Press, 2009, pp. 465 -494.

[2] J. A. Parker, R. V. Kenyon and D. E. Troxel, "Comparison of interpolation methods for image resampling," *IEEE Transactions on Medical Imaging*, Vols. MI-2, no. 1, pp. 31 - 39, 1983.

[3] E. Meijering, "A chronology of interpolation: From ancient astronomy to modern signal and image processing," *Proceedings of the IEEE*, vol. 90, no. 3, pp. 319-342, 2002.

[4] R. G. Keys, "Cubic convolution interpolation for digital image processing," *IEEE Transactions on Acoustics, Speech and Signal Processing*, Vols. ASSP-29, no. 6, pp. 1153 - 1156, 1981.

[5] P.-S. Tsai and T. Acharya, "Image up-sampling using discrete wavelet transform," in *Proceedings of The 2006 Joint Conference on Information Sciences*, Kohsiung, Taiwan, October, 2006.

[6] A. Temizel and T. Vlachos, "Wavelet domain image resolution enhancement using cycle spinning and edge modelling," in *The 13th European Signal Processing Conference (EUSIPCO 2005)*, Antalya, Turkey, September, 2005.

[7] H. Demirel and G. Anbarjafari, "Image resolution enhancement by using discrete and stationary wavelet decomposition," *IEEE Transactions on Image Processing*, vol. 20, no. 5, pp. 1458-1460, 2011.

[8] S. Naik and N. Patel, "Single image super resolution in spatial and wavelet domain," *The International Journal of Multimedia and its Applications*, vol. 5, no. 4, pp. 23-32, 2013.

[9] R. P. Bagawade, K. S. Bhagawat and P. M. Patil, "Wavelet transfrom techniques for image resolution enhancement: A study," *International Journal of Emerging Technology and Advanced Engineering*, vol. 2, no. 4, pp. 167 - 172, 2012.

[10] N. Tripathi and K. G. Kirar, "Image resolution enhancement by wavelet transform based interpolation and image fusion," *International Journal of Advanced Research in Computer Science and Software Engineering*, vol. 4, no. 8, pp. 318 -323, 2014.

[11] S.-C. Tai, T.-M. Kuo, C.-H. Iao and T.-W. Liao, "A fast algorithm for single image super resolution in both wavelet and spatial domain," in *International Symposium on Computer, Consumer and Control*, Taichung, Taiwan, 2012.

[12] A. Garg, S. V. Naidu, H. Yahia and D. Singh, "Wavelet based resolution enhancement for low resolution satellite images," in *9th International Conference on Industrial and Information Systems (ICIIS)*, Gwalior, India, 2014.

[13] W. K. Carey, D. B. Chuang and S. S. Hemami, "Regularity - preserving image interpolation," *IEEE Transaction on Image Processing*, vol. 8, no. 9, pp. 1293-1297, 1999.

[14] H. Chavez-Roman and V. Ponomaryov, "Super resolution image generation using wavelet domain interpolation with edge extraction via sparse representation," *IEEE Geoscience and Remote Sensing Letters*, vol. 11, no. 10, pp. 1777-1781, 2014.

[15] V. I. Ponomaryov, H. Chavez-Roman and V. Gonzalez-Huitron, "Image resolution enhancement using edge extraction and sparse representation in wavelet domain for real-time application," in *Real-Time Image and Video Processing 2014*, Brussels, Belgium, 2014.

[16] O.-J. Kwon and J.-H. Park, "Region adaptive single image super resolution using wavelet transfrom," *International Journal of Multimedia and Ubiquitous Engineering*, vol. 9, no. 12, pp. 249-258, 2014.

[17] M. Irani and S. Peleg, "Motion analysis for image enhancement: resolution, occlusion and transparency," *Journal of Visual Communication and Image Representation*, vol. 4, no. 4, p. 324–335, 1993.

[18] S. Dai, M. Han, Y. Wu and Y. Gong, "Bilateral back-projection for single image super resolution," in *IEEE International Conference on Multimedia and Expo*, Beijing, China, July, 2007.

[19] P. Shreyas A., "Novel iterative back projection approach," *IOSR Journal of Computer Engineering*, vol. 11, no. 1, pp. 65-69, 2013.

[20] Q. Zhou, S. Chen, J. Liu and X. Tang, "Edge-preserving single image super-resolution," in *ACM Multimedia Conference 2011*, Scottsdale, Arizona, USA, November - December, 2011.

[21] Z. Wang, "The SSIM Index for Image Quality Assessment," New York University, 11 February 2011. [Online]. Available: www.cns.nyu.edu/lcv/ssim. [Accessed 25 November 2014].

[22] X. Li and M. T. Orchard, "New edge directed interpolation," *IEEE Transactions on Image Processing*, vol. 10, no. 10, pp. 1521 - 1527, 2001.

[23] R. C. Gonzalez and R. E. Woods, Digital Image Processing, 3 ed., New Jersey: Prentice-Hall, 2008.

[24] S. C. Park, M. K. Park and M. G. Kang, "Super-resolution image reconstruction: A technical overview," *IEEE Signal Processing Magazine*, vol. 20, no. 3, pp. 21-36, 2003.